Supporting Information

Kang et al. 10.1073/pnas.1320401111

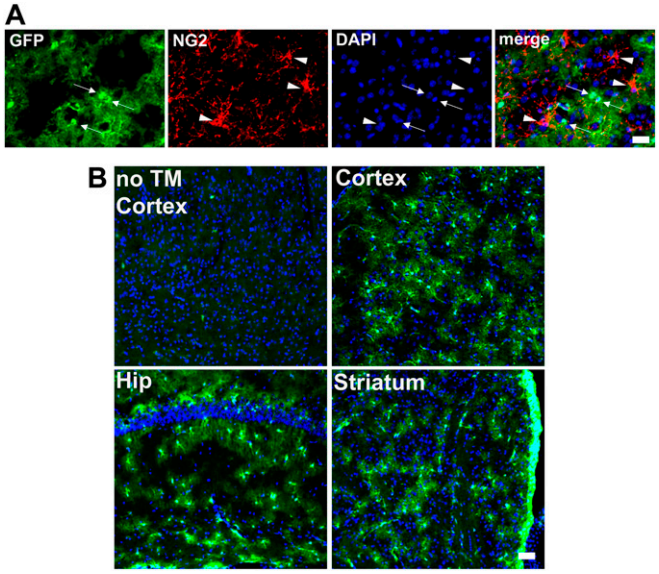

Fig. S1. (*A*) Two weeks after tamoxifen ™ treatment of *Nestin-CreER;Rosa26*$^{lox\text{-}stop\text{-}lox\text{-}EGFP}$ mice, GFP^{+} cells (green, arrows) colabeling with NG2^{+} precursor cells (red, arrowheads) cannot be detected. (Scale bar: 20 μm.) (*B*) *Nestin-CreER* confers recombination in astrocytes in the adult cerebrum. Immunostaining for GFP in tissues from *Nestin-CreER;Rosa26*$^{lox\text{-}stop\text{-}lox\text{-}EGFP}$ mice 2 wk (as well as 1 and 17 wk, not shown) after TM treatment reveals GFP^{+} cells with typical astrocyte morphology (small nucleus and fine processes) in the neocortex, striatum, and hippocampus. Brain tissues from the same genotype but without TM treatment show no GFP^{+} cells. Note that GFP^{+} cells were also detected as expected in neural precursors in the neurogenic regions of the cerebrum, including the anterior subventricular zone, dentate gyrus, rostral migratory stream, and olfactory bulb (not shown). (Scale bar: 50 μm.)

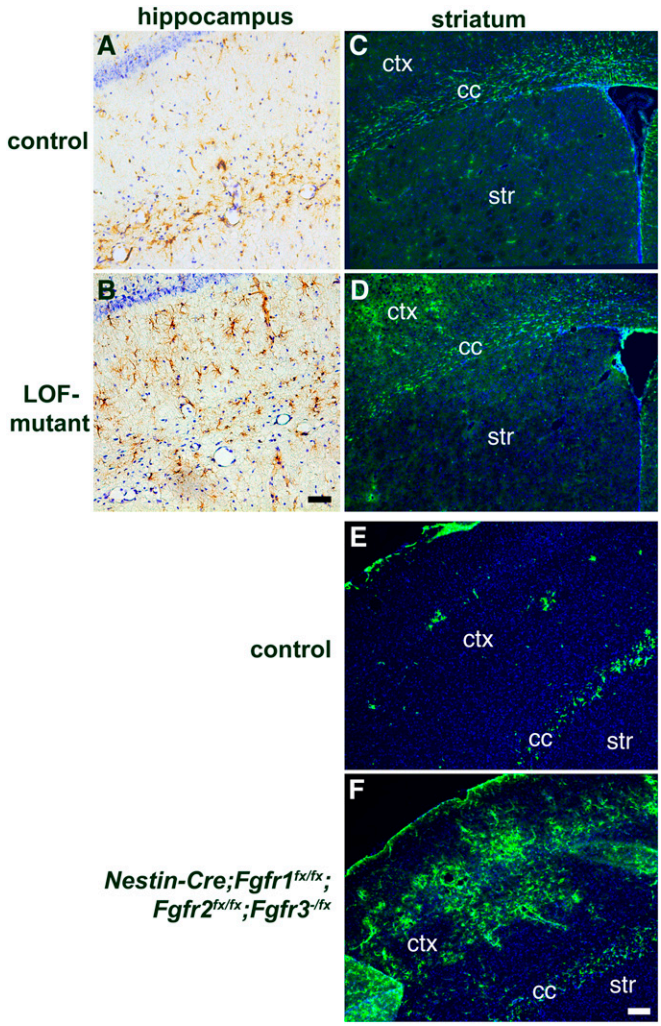

Fig. S2. Loss of FGF signaling leads to astrogliosis in the hippocampus but not the striatum. (*A* and *B*) Compared with the control, the loss-of-function (LOF) mutant hippocampus exhibits strong immunostaining for GFAP (brown) and hypertrophic astrocytes 4 wk after TM treatment. Blue cells in upper left corner are CA1 neurons. (Scale bar: 20 μm.) (*C* and *D*) Interestingly, $GFAP^{+}$ astrocytes (green) were not present in the striatum (str) in the mutant, suggesting a difference in the requirement for FGF signaling between dorsal and ventral areas of the cerebrum. (*E* and *F*) Compared with the LOF mutants, in which *Fgfr3* is null, the increase in GFAP expression is similar in mutants in which *Fgfr3* is also conditionally deleted. cc, corpus callosum, ctx, neocortex. (Scale bars: *C–F*, 50 μm.)

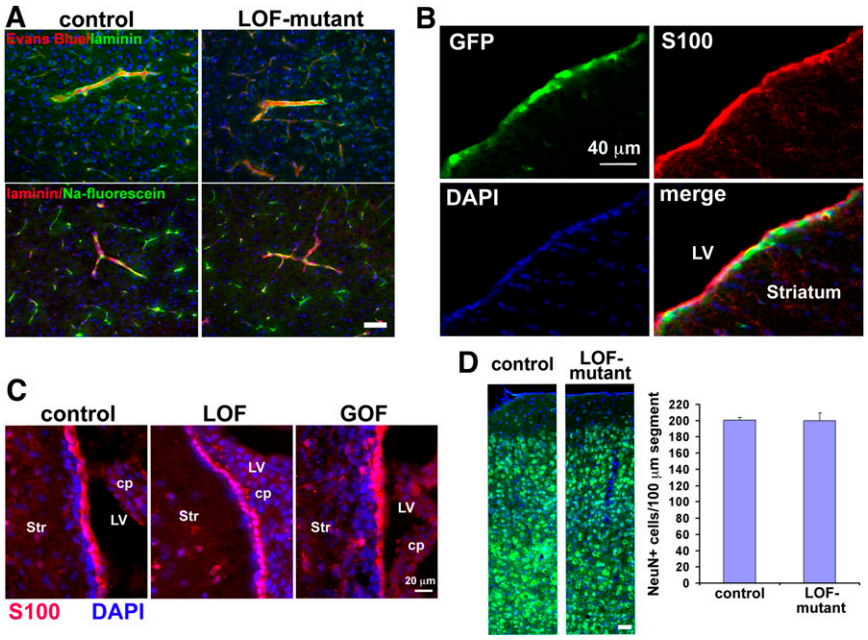

Fig. S3. Loss of FGF signaling in cortical astrocytes does not disrupt the blood–brain barrier, lead to gross ependymal layer defects, or lead to neuronal degeneration. (*A*) Three weeks after TM treatment, the fluorescence tracers Evans blue (30 kDa) and sodium fluorescein (0.3 kDa) were found restricted inside the blood vessel lumen, immunostained for the endothelial marker laminin, in the LOF-mutant neocortex. (Scale bar: 50 μm.) (*B*) Two weeks after TM treatment of *Nestin-CreER*;*Rosa26*$^{lox\text{-}stop\text{-}lox\text{-}EGFP}$ mice, ependymal cells (S100^{+}, red) are recombined (GFP^{+}). (*C*) The ependymal cell layer (S100^{+}, red) appears grossly normal in both LOF and gain-of-function (GOF) mutants. cp, choroid plexus; LV, lateral ventricle; Str, striatum. (*D*) Immunostaining for the neuronal marker NeuN (green) does not reveal a difference in the numbers, density, or distribution of neurons between LOF mutants and controls 2 mo after TM treatment. NeuN^{+} cells were counted in 100-μm-wide segments of neocortex from pia to corpus callosum in positionally matched sections. (Scale bar: 50 μm.)

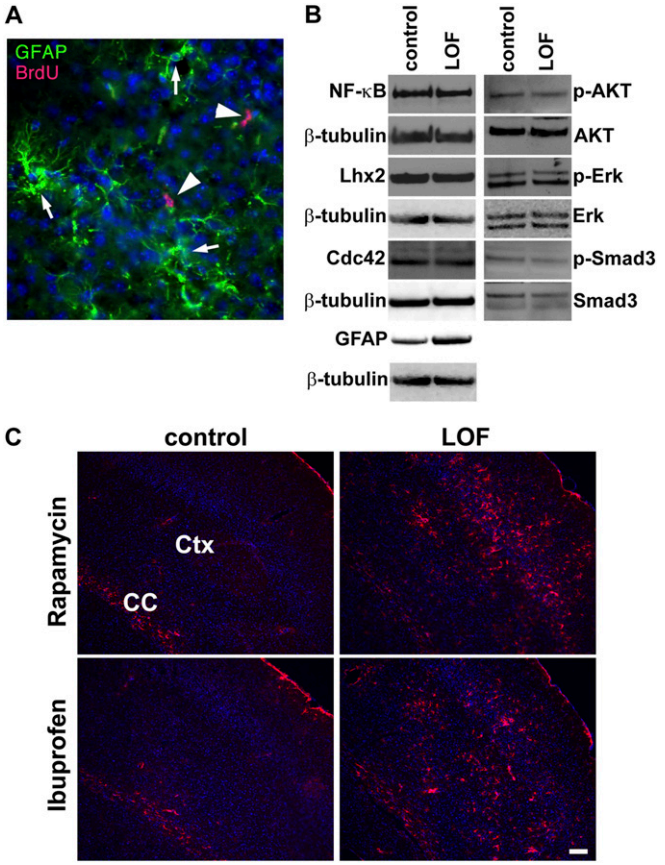

Fig. S4. (*A*) Reactive astrocytes are not newly generated cells. Reactive astrocytes stained for GFAP (green, arrows) do not label with BrdU (red, arrowheads) 30 d after BrdU was administered (100 mg/kg body weight) three times a day for 3 d starting on the last day of TM injections. (*B*) Western blot of LOF mutants 4 wk after TM treatment does not reveal a difference in the levels of candidate factors involved in FGF signaling (pAKT, pERK) or in the activation of astrocytes (NF-κB, Lhx2, Cdc42, pSmad3). (*C*) Coronal sections through the cortex of LOF and control mice treated with rapamycin or ibuprofen indicate that reactive astrocytes ($GFAP^+$, red) are still present. Sections are counterstained with Hoechst (blue). (Scale bar: 100 μm.)

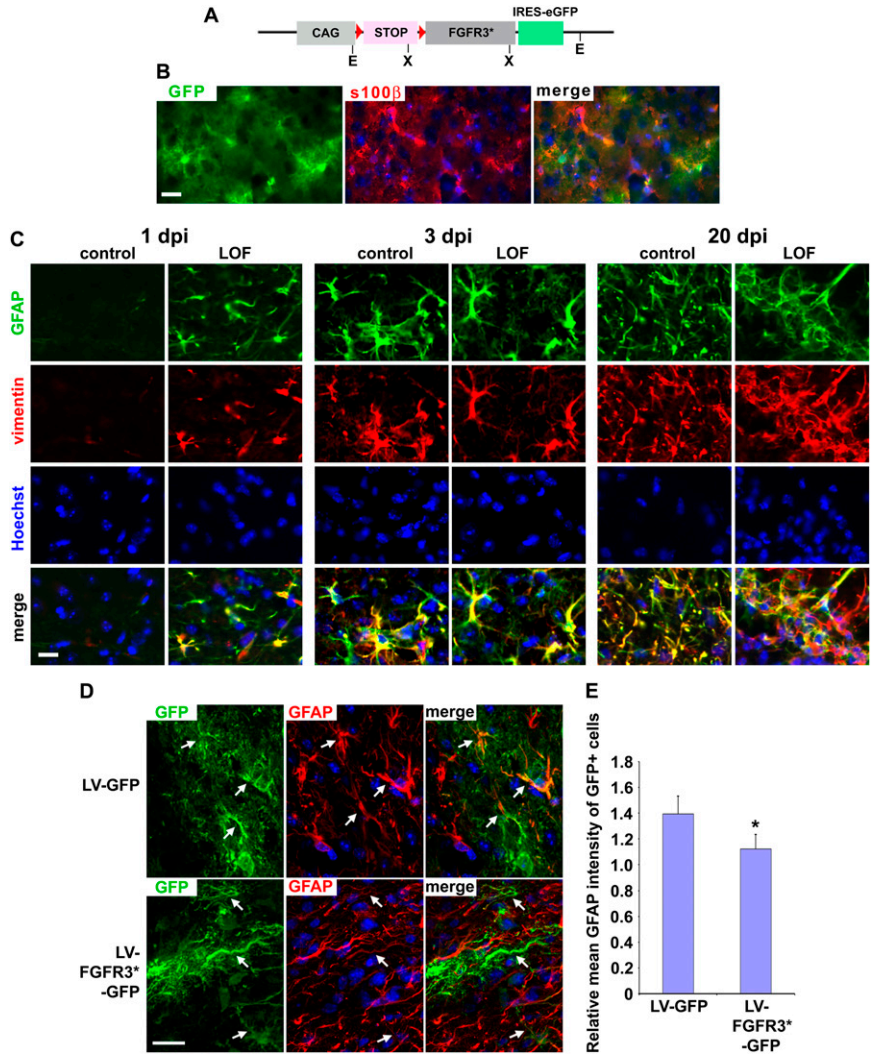

Fig. S5. Constitutively active FGFR3 inhibits GFAP expression in astrocytes upon cortical injury. (*A*) Generation of the FGFR3 GOF mutant. The cDNA sequence encoding a constitutively active form of FGFR3, FGFR3TDII^{K650E}, with an IRES-eGFP was placed under the ubiquitous CAG promoter with a floxed STOP sequence in between (*Materials and Methods*). Red arrowheads represent the lox sites. (*B*) In Nestin-CreER;GOF mutants, recombination in the neocortex is restricted to astrocytes. Colabeling with anti-GFP and anti-s100β reveals that GFP$^+$ cells are characteristic bush-like s100β$^+$ astrocytes 3 wk after TM treatment. (Scale bar: 20 μm.) (*C*) At 1, 3, and 20 d after stab wound injury [i.e., days post injury (dpi)], astrocytes that are GFAP$^+$ (green) are also vimentin$^+$ (red) in controls and LOF mutants. (Scale bar: 20 μm.) (*D*) Lentiviral expression of a constitutively active FGFR3 mutant inhibits GFAP expression in astrocytes upon cortical injury of WT mice. In this case, the viral injection itself provides the injury. Coimmunofluorescence with anti-GFP and anti-GFAP revealed reduced GFAP staining in GFP$^+$ astrocytes around the injection sites in LV-FGFR3*-GFP infected brains compared with LV-GFP infected brains 2 wk after injection. Arrow indicates colabeled cells. (Scale bar: 20 μm.) (*E*) Quantification of GFAP immunointensity confirms reduced GFAP expression in GFP$^+$ astrocytes infected with LV-FGFR3*-GFP virus (*Materials and Methods*). The counterstain is Hoechst. The graphs represent ratios relative to the mean value obtained for controls, which was set as 1 (mean ± SEM; $*P < 0.05$ and $**P < 0.001$).

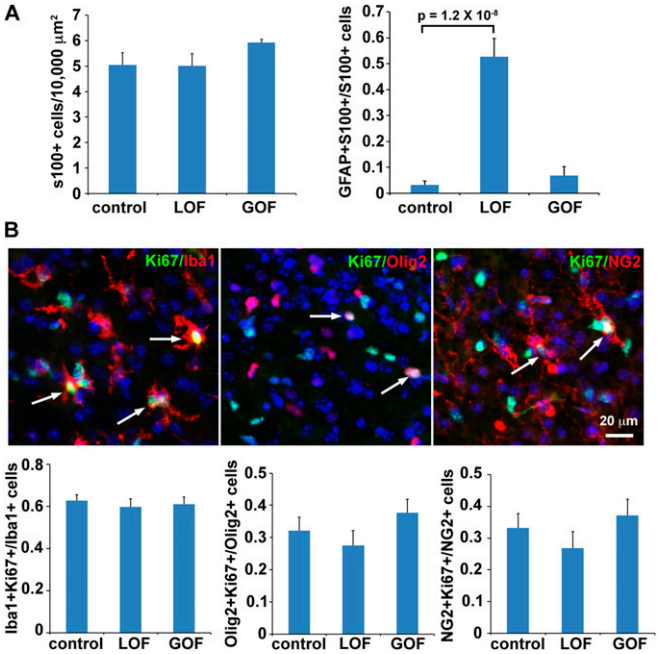

Fig. S6. (*A*) At 1 d post injury, the number of astrocytes immediately adjacent to the lesion is not different between mutants (LOF and GOF) and controls, but the proportion of astrocytes expressing GFAP is significantly increased in LOF mutants. (*B*) At 3 d post injury, the ratio of Ki-67^{+} (green) cells that are Iba1^{+} microglia, Olig2^{+} cells, or NG2^{+} cells (red, arrows) is not significantly different between mutants (LOF and GOF) and controls ($n \geq 3$ for each genotype for each stain).

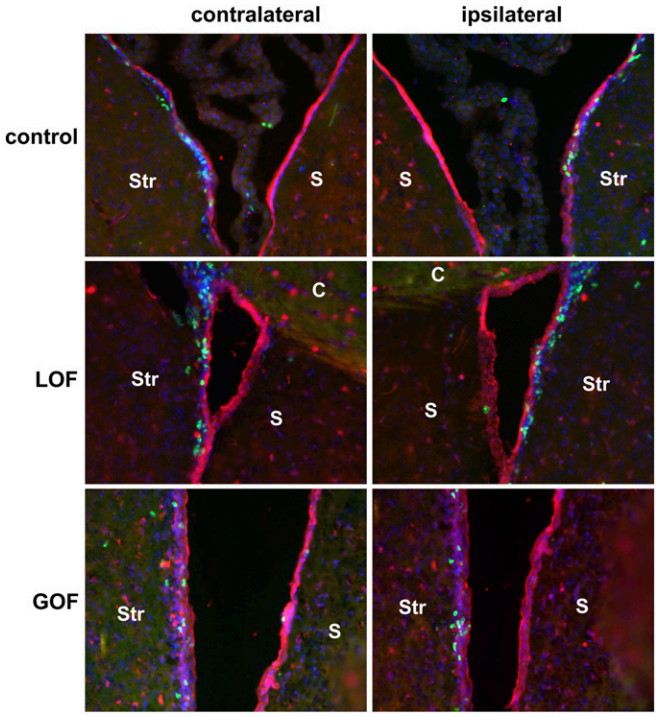

Fig. S7. Ependymal cells do not acquire expression of the proliferation marker Ki-67 upon injury. Ependymal cells are labeled with S100 (red) and proliferating cells with Ki-67 (green) in sections that encompass the lateral ventricles of each hemisphere, contralateral and ipsilateral to the injury side. The subventricular zone, which is immediately adjacent to the ependymal layer on the striatal side (Str) of the ventricles, provides an internal positive control for proliferating Ki-67^{+} cells. Sections are counterstained with DAPI (blue). C, cortex; S, septum.

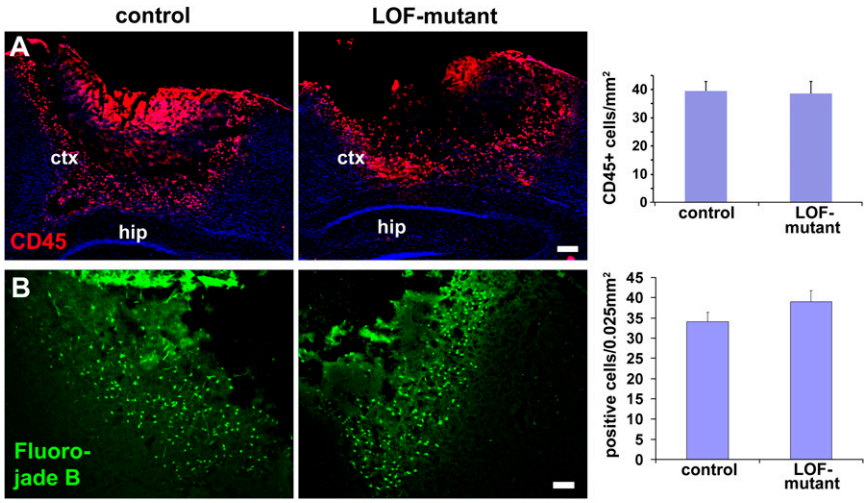

Fig. S8. Loss of FGF signaling does not influence the injury-induced inflammatory response and neuron degeneration. (*A*) In coronal sections, leukocytes marked by anti-CD45 labeling are restricted to the lesion area in the control and LOF mutant 3 d after injury. ctx, neocortex; hip, hippocampus. (Scale bar: 200 μm.) (*B*) Degenerating neurons stained by Fluoro-Jade B were found in comparable numbers around the injury sites in controls and LOF mutants 1 d after injury. Cells were counted within 100-μm-wide radial segments (250 μm long) at the distal tip of the injury and halfway up both sides for at least three sections per animal. (Scale bar: 50 μm.)